*Inorg. Chem.* **2007**, *46*, 8859–8870


# Rates of Electronic Excitation Hopping in Anisotropic Ionic Crystals of [Ru(2,2′-bipyridine)$_3$]X$_2$ (X = $ClO_4^-$, $PF_6^-$, $SbF_6^-$); Monte Carlo Simulation of Single- and Multi-Exponential Emission Decays

**Takeshi Ohno,* Koichi Nozaki, Mayuko Nakamura, Yoshiaki Motojima, Minoru Tsushima, and Noriaki Ikeda***

*Department of Chemistry, Graduate School of Science, Osaka University, 1-16 Machikaneyama, Toyonaka, Osaka 560-0043, Japan*

Received May 31, 2006

Emission decays of triplet metal-to-ligand charge transfer states in anisotropic crystals of [$Ru_{1-x}Os_x$(bpy)$_3$]X$_2$ (bpy = 2,2′-bipyridine, X = $PF_6^-$, $ClO_4^-$, $SbF_6^-$, and 0.115 > $x$ > 0.001) at ∼300 K were measured by means of time-correlated single-photon counting. Rates of excitation hopping calculated on the basis of an interaction between transition dipoles of a donor cation and an acceptor cation are insufficient to simulate the single-exponential decays ($x$ = 0.0099) and the multiexponential decays ($x$ = 0.060 and 0.115) of the $PF_6^-$ salt crystals. A limiting rate of excitation hopping to an imaginary cation at the van der Waals distance via a super-exchange interaction between d orbitals through the bpy ligands was determined to be $0.83 \times 10^{10}$ s$^{-1}$ on average by means of a step-by-step Monte Carlo simulation, assuming an distance-attenuation factor, $\beta$, of the exchange interaction of 10 nm$^{-1}$. The total rate of excitation hopping via both a dipole–dipole mechanism and a super-exchange mechanism to the neighboring sites of the cation was calculated to be $5.4 \times 10^9$ s$^{-1}$ for the $PF_6^-$ crystal. Anisotropic diffusion constants estimated from the hopping rates and lengths in the $PF_6^-$ crystal are $9.3 \times 10^{-6}$, $9.1 \times 10^{-6}$, and $1.4 \times 10^{-6}$ cm$^2$s$^{-1}$ along the *a* axis, the *b* axis, and the *c* axis, respectively, which are compared with an isotropic diffusion constant, $1.3 \times 10^{-6}$ cm$^2$ s$^{-1}$, estimated from the pseudo-bimolecular rate constant of excitation transfer to [Os(bpy)$_3$]$^{2+}$, using an isotropic Smoluchowski equation. A multiexponential emission decay of [$Ru_{0.885}Os_{0.115}$(bpy)$_3$](PF$_6$)$_2$ was also simulated to determined the limiting rate of excitation transfer to [Os(bpy)$_3$]$^{2+}$ at the van der Waals distance ($2.6 \times 10^{11}$ s$^{-1}$). The magnitude of $\beta$ determined is 6.5 and 11.5 nm$^{-1}$ for the $ClO_4^-$ and the $SbF_6^-$ salt crystals, respectively, on reference to that of $\beta$ (10 nm$^{-1}$) for the $PF_6^-$ salt crystal.

## Introduction

Transport of excitation energy through a crystalline solid, which is called excitation migration, competes with the intrinsic emission of light, conversion to heat, and chemical conversion of the host species to a more-mobile species (an electron and a hole) and a decomposed or isomerized species of the host. Fluorescent states of anisotropic organic molecular crystals such as anthracene exhibit strong intermolecular interactions because of their large transition moments and are described as excitons that are bound to more than two molecules.[1,2] As a result of the strong intermolecular interactions, the singlet excitation energy migrates with a diffusion constant of $3 \times 10^{-3}$ cm$^2$ s$^{-1}$ along the *a* axis of an anthracene crystal.[3] Triplet excitation energy of an anisotropic anthracene crystal migrates with a diffusion constant of $1.5 \times 10^{-4}$ cm$^2$ s$^{-1}$ along the *a* axis[4] because of weak dipole−dipole and exchange interactions. Rates of 3D excitation migration in anisotropic crystals of metal coordination compounds have been rarely studied except for the migration of the triplet electronic excited states of metal-to-ligand charge transfer in anisotropic crystals of Pd(6-Phenyl-bpy)Cl,[5] [Ru(bpy)$_3$](PF$_6$)$_2$,[6−8] and [Os(bpy)$_3$](PF$_6$)$_2$,[9] the quintet

* To whom correspondence should be addressed. E-mail: ohno@ch.wani.osaka-u.ac.jp.

(1) Pope, M.; Swenberg, C. *Electronic Processes in Organic Crystals and Polymers*; 2nd ed.; Oxford University Press: Oxford, U.K., 1999.
(2) Knox, R.S. *Theory of Excitons*; Acadmic Press: New York, 1963.
(3) Wolf, H. C. *Advances in Atomic and Molecular Physics*; Academic Press: New York, 1967; p 119. (*Z. Naturforsch* **1958**, *A13*, 414.)
(4) Ern, V. *Phys. Rev. Lett.* **1969**, *22*, 8.
(5) Karlen, T.; Ludi, A.; Güdel, H. U.; Riesen, H. *Inorg. Chem.* **1991**, *30*, 2250.
(6) Braun, D.; Yersin, H. *Inorg. Chem.* **1995**, *34*, 1967.

10.1021/ic060948f CCC: $37.00 
Published on Web 09/14/2007

electronic excited state of the Cr(III) dimer in an anisotropic crystal of $[(NH_3)_5CrOHCr(NH_3)_5]Cl_5 \cdot H_2O$[10], and the doublet electronic-excited-state of Cr(III) in the cubic crystal of $[Cr(bpy)_3][NaCr(ox)_3]ClO_4$ (bpy = 2,2′-bipyridine, ox = oxalate ion).[11,12]

The rate of excitation hopping to the nearest (0.506 nm) metal sites in the anisotropic crystal of Pd(6-phenyl-bpy)Cl was estimated to be $10^{11}$ $s^{-1}$ from the observed rate of transfer to Pt(6-phenyl-bpy)Cl impurity.[5] Rates of excitation hopping to the closest (0.819 nm) sites along the *c* axis and the second-closest (1.076 nm) sites along the *a* and *b* axes in anisotropic crystals of $[Ru(bpy)_3](PF_6)_2$ doped with $[Os(bpy)_3](PF_6)_2$ at ~300 K were estimated to be $3.6 \times 10^8$ and $0.18 \times 10^8$ $s^{-1}$ through the use of a step-by-step Monte Carlo simulation of multiexponential emission decays.[7] A similar value of the hopping rate ($4 \times 10^8$ $s^{-1}$) at ~300 K was obtained on the basis of the pseudo-bimolecular rate constant of Ru-to-Os excitation transfer in the $[Ru_{1-x}Os_x(bpy)_3](PF_6)_2$ crystal, without respect to the anisotropy of the crystal.[8] Small diffusion constants of excitation migration, $((1.3-4.6) \times 10^{-6}$ $cm^2$ $s^{-1})$ were roughly estimated on the basis of an isotropic bimolecular rate equation of Smoluchowski, the hopping rate, and the closest site−site distance for $[Ru_{1-x}Os_x(bpy)_3]X_2$ crystals (X = $PF_6^-$, $ClO_4^-$, $Cl^-$). Excitation hopping in the neat crystal of $[Ru(bpy)_3](PF_6)_2$ and in the homo layer of $[Os(bpy)_3](PF_6)_2$ below 4 K have been also pursued by Yersin et al.[6,9] by means of time- and energy-resolved emission spectroscopy. Weakly exothermic excitation transfer between sites in the $[Ru(bpy)_3](PF_6)_2$ crystal, in which the emitting states are split due to the lowered space symmetry of the crystal below 105 K was observed to occur at a rate of $1.6 \times 10^7$ $s^{-1}$.[6] Similarly, the site−site excitation transfer is so rapid that emission comes from the lowest energy site of $[Os(bpy)_3](PF_6)_2$ in the homochiral layers of $\{\Lambda$-$[Ru(bpy)_3]\Delta$-$[Os(bpy)_3]\}(PF_6)_4$.[9] The rate of site-to-site excitation hopping is slower ($\sim 1 \times 10^8$ $s^{-1}$) than that of the intramolecular bpy-to-bpy excitation transfer of $[Ru(bpy)_3]^{2+}$ doped in $[Zn(bpy)_3](ClO_4)_2$, as determined by means of time-resolved luminescence line-narrowing by Riesen et al.[13]

To understand excitation hopping in anisotropic ionic crystals of coordination compounds, the preliminary studies[7,8] on the hopping rate in $[Ru(bpy)_3]X_2$ (X = $ClO_4^-$, $PF_6^-$, $SbF_6^-$) at ~300 K should be reinvestigated by carefully taking into account the crystallographic data of the distances and configurations between the cations. Both the anions and the ligands are anticipated to cause a variation in the distance and configuration parameters of the cations and to tune the diffusional motion of excitation in the crystals. The cations are generally spherical with some ligand projections and can accommodate a number of anions with various sizes and shapes, all of which creates an anisotropic structure of the crystal. The sizes and shapes of the anions, therefore, modify the extent of intermolecular interaction, resulting in anisotropic excitation diffusion in the same way that the anisotropic crystal structures of planar organic molecules exhibit an anisotropic diffusion constant of excitation.[4]

Exponential decays of emission with a time-dependent rate constant in an inhomogeneous or anisotropic environment have been simulated to obtain the rates of excitation hopping and excitation transfer simultaneously through the use of a step-by-step Monte Carlo simulation,[7] which has been shown to be an effective method to assess the rates of quenching by dense impurities in crystals or in liquid crystals,[14−17] In this article, a step-by-step Monte Carlo simulation was applied to both the multiexponential decay and the single-exponential decay of electronic excitation. Single-exponential emission decays of $[Ru_{1-x}Os_x(bpy)_3]^{2+}$ ($x < 0.01$) were analyzed to determine the rates of excitation hopping to the neighboring Ru(II) cations by means of a step-by-step Monte Carlo simulation; the multiexponential emission decay of $[Ru_{1-x}Os_x(bpy)_3]^{2+}$ ($x > 0.06$) was simulated to assess the rates of excitation transfer to the Os(II) cations at the close sites. A step-by-step Monte Carlo simulation of the single-exponential emission decay leads to an estimate of a maximum value of $9.3 \times 10^{-6}$ $cm^2$ $s^{-1}$ for the anisotropic diffusion constant of excitation in crystals of $[Ru_{1-x}Os_x(bpy)_3](PF_6)_2$ from the rate and length of hopping, by taking the anisotropy in the crystal into account.

## Experimentals Section

**Materials.** $[M(bpy)_3](ClO_4)_2$, $[M(bpy)_3](PF_6)_2$, and $[M(bpy)_3](SbF_6)_2$, (M = Ru and Os) were prepared by metathesis from $[Ru(bpy)_3]Cl_2 \cdot 7H_2O$,[18] and $[Os(bpy)_3]I_2$[19] or $[Os(bpy)_3]Cl_2 \cdot 6H_2O$,[20] respectively, according to literature methods and then recrystallized from acetonitrile-ethanol solution. The crystals of $[Ru(bpy)_3]X_2$ doped with $[Os(bpy)_3]X_2$ were prepared by following the preparation method[7] of $[Ru(bpy)_3](PF_6)_2$ doped with $[Os(bpy)_3](PF_6)_2$ from acetonitrile-ethanol solution, after mixing the solution of each component in the stoichiometric molar ratio. The doping concentration of the highly doped crystal was determined by measuring the absorption spectra of the solution in which the doped crystal was redissolved.

**Measurement of Emission Decays.** A time-correlated single-photon counting system[7] was used to measure the decays of emission at $16.6 \times 10^3$ $cm^{-1}$ and at 299 ± 2 K. The light source was a Kerr lens mode-locked $Ti^{3+}$:sapphire laser with a cavity dumper, which consists of a fused-silica Bragg Cell (Harris H101)


(7) Tsushima, M.; Ikeda, N.; Nozaki, K.; Ohno, T. *J. Phys. Chem. A* **2000**, *104*, 5176.
(8) Ikeda, N.; Yoshimura, A.; Tsushima, M.; Ohno, T. *J. Phys. Chem. A* **2000**, *104*, 6158.
(9) Breu, J.; Kratzer, C.; Yersin, H. *J. Am. Chem. Soc.* **2000**, *122*, 2548.
(10) Riesen, H.; Guedel, H.U. *Mol. Phys.* **1986**, *58*, 509.
(11) von Arx, M. E.; Hauser, A.; Riesen. H.; Pellaux, R.; Decurtins, S. *Phys. Rev. B* **1996**, *54*, 15800.
(12) von Arx, M. E.; Langford, V. S.; Oetliker, U.; Hauser, A. *J. Phys. Chem. A* **2002**, *106*, 7099.
(13) Riesen, H.; Gao, U.; Krausz, E. *Chem. Phys. Lett.* **1994**, *228*, 610.
(14) Markovitsi, D.; Germain, A.; Millie, P.; Lecuyer, P.; Gallos, L. K.; Argyrakis, P.; Bengs, H.; Ringsdorf, H. *J. Phys. Chem.* **1995**, *99*, 1005.
(15) Goulet, T.; Fraser, M.-J.; Frongillo, Y.; Jay-Gerin, J.-P. *Radiat. Phys. Chem.* **1998**, *51*, 85.
(16) Yatskou, M. M.; Donker, H.; Novikov, E. G.; Koehorst, R. B. M.; van Hoek, A.; Apanasovich, V. V.; Schaafsma, T. J. *J. Phys. Chem. A* **2001**, *105*, 9498.
(17) Diaj-Torres, I. A.; Barbosa-Garcia, O.; Struck, C. W.; McFarlane, R. A. *J. Lumin.* **1998**, *78*, 69.
(18) Palmer, R. A.; Piper, T. S. *Inorg. Chem.* **1966**, *5*, 864.
(19) Burstall, F. P.; Dwyer, F. P.; Gyarfus, E.C. *J. Chem. Soc.* **1950**, 953.
(20) (a) *Inorg. Synth.* **1986**, *XXIV*, 291. (b) Johnson, S. R.; Westmoreland, T. D.; Caspar, J.V.; Barqawi, K. R.; Meyer, T. J. *Inorg. Chem.* **1988**, *27*, 3195.

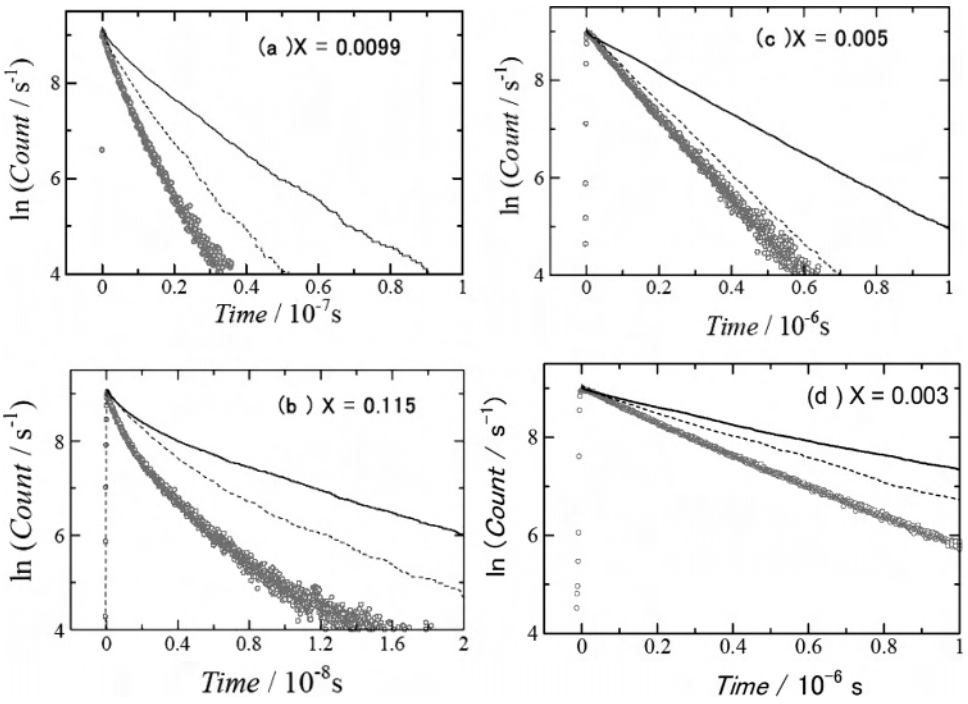


**Figure 1.** Observed emission decays (gray circles) and simulated emission decays (solid lines with a $\tau_o$ of 15 $\mu$s and broken lines with a $\tau_o$ of 6.5 $\mu$s) based on the dipole−dipole mechanism of excitation-energy transfer for the $PF_6^-$, $ClO_4^-$, and $SbF_6^-$crystals of $[Ru_{1-x}Os_x(bpy)_3]X_2$. (a) The $PF_6^-$ crystal with an $x$ of 0.0099 (b) the $PF_6^-$ crystal with an $x$ of 0.115, (c) the $ClO_4^-$crystal with an $x$ of 0.005, and (d) the $SbF_6^-$crystal with an $x$ of 0.003.

and a radio frequency wave driver (CAMAC CD5000) with a booster amplifier (CAMAC PB1800), yielding a 10−20 nJ/pulse at 800 nm with a repetition rate of 200 kHz. The laser output pulse was frequency doubled to 400 nm using a BBO crystal (Type I, 2 mm thick). The intensity of the 400 nm laser was 3 nJ with an area of 0.06 cm$^2$ (50 nJ/cm$^2$), which is small enough to prevent the appearance of the bimolecular annihilation of the triplet metal-to-ligand charge transfer (MLCT) state of a neat crystal.[7]

Emission from the samples was detected with a monochromator (Jobin Yvon HR 10) with a microchannel plate photomultiplier (MCP−PM Hamamatsu R3809U-51X) that was cooled. Signals from a high-speed photodiode (Hamamatsu C4258) of the start pulse and the MCP−PM of the stop pulse were amplified with preamplifiers (EG&G Ortec VT120B and 9306, respectively) and then discriminated with a ps-timing discriminator (EG&G Ortec 9307). Those output pulses were fed into a time-to-amplitude converter (TAC, EG&G Ortec 567). The output of the TAC was transferred to a computer for data storage, display, and analysis. The full width at half-maximum (fwhm) of the instrumental response function (IRF) is typically 40 ps.

## Results and Discussion

**1. Emission Decays of $[Ru_{1-x}Os_x(bpy)_3]X_2$. 1−1. Single-Exponential Emission Decays of $[Ru_{1-x}Os_x(bpy)_3]X_2$ crystals (X = $CO_4^-$, $PF_6^-$, $SbF_6^-$) (0.01 < x).**

Most of the $^3$CT(Ru) emissions of $[Ru_{1-x}Os_x(bpy)_3]X_2$ ($x$ < 0.01) at 16.6 × 10$^3$ cm$^{-1}$ were observed to decay in an almost single-exponential manner across the whole time range as shown in parts a, c, and d of Figure 1. The rates of the single-exponential decays were almost linearly proportional to the concentration of $[Os(bpy)_3]X_2$ doped in a $[Ru(bpy)_3]X_2$ crystal. The pseudo-bimolecular rate constant of emission quenching in the $[Ru(bpy)_3]X_2$ crystal (shown in Table 1) was obtained by plotting the observed decay rate constants against the $Os^{2+}$ concentration, as was shown in the previous work.[8] That the $[Os(bpy)_3]X_2$ in the mixed crystals accepts the excitation energy of $[Ru(bpy)_3]X_2$ (17.5 × 10$^3$ cm$^{-1}$) was ascertained by a gradual increase in the intensity of the low-energy emission of $[Os(bpy)_3]X_2$ (<14.5 × 10$^3$ cm$^{-1}$) after the pulse-laser excitation.[8] The linear dependence of the decay rate on the concentration of $[Os(bpy)_3]X_2$ unquestionably shows that the migration of electronic excitation occurs through the host crystal followed by excitation transfer to $[Os(bpy)_3]X_2$, which exists as an energy sink in the crystal. Provided that isotropic excitation migration takes place despite their anisotropic crystal structures (hexagonal or monoclinic), the rate constant of the pseudo-bimolecular excitation transfer process ($k_{ent}$) could be written by the Smoluchowski equation of bimolecular reaction,[20]

$$k_{ent} = 4\pi D R_{eff} N_o \quad (1)$$

where $D$, $R_{eff}$, and $N_o$ are the diffusion constant of electronic excitation in the crystal, the largest collision diameter of the exclusive Ru-to-Os excitation transfer, and Avogadro's number, respectively. By assuming the collision diameter for exclusive excitation transfer to an Os(II) ($R_{eff}$) to be the

**Table 1.** Bimolecular Rate Constant, $k_{ent}$, Exclusive Reactive Distance, $R_{eff}$, and Diffusion Constants, $D$, of Excitation Transfer in the Crystals of $[Ru(bpy)_3]X_2$

| X | $k_{ent}$ $10^{11}$mol$^{-1}$cm$^{-3}$s$^{-1}$ | $R_{eff}$ nm | $D$ $10^{-6}$cm$^2$s$^{-1}$ |
|---|---|---|---|
| $ClO_4^-$ | 37[a] | 1.076[c] | 2.7 |
| $PF_6^-$ | 10.8[a] | 1.076[d] | 1.3 |
| $SbF_6^-$ | 4.4[b] | 1.083[b] | 0.54[b] |

[a] Ref 8. [b] This study. [c] Ref 22. [d] Ref 23.

second-closest site−site distance in the host crystal, the magnitudes of $D$ were calculated to be in the range of $0.54 \times 10^{-6}$ and $3.1 \times 10^{-6}$ cm$^2$ s$^{-1}$, as shown in Table 1.[8] The magnitudes of $D$ are smaller than the molecular diffusion constants of polar and nonpolar solvents by 1 or 2 orders of magnitude and smaller than the excitation diffusion constants in organic crystals (such as anthracene[4]) by 2 or 3 orders of magnitude. In a qualitative sense, the excitation of $[Ru(bpy)_3]^{2+}$, which is bound to one site of the cation, jumps to one of the near sites with the help of the intermolecular exchange interactions of electron and hole[24] and dipole−dipole interactions.[25]

The rate constant of excitation hopping to the closest sites, $k$, can be evaluated for the $PF_6^-$ salt crystal by assuming the isotropy of the crystal. The hopping rate constant is calculated to be $6 \times 10^8$ s$^{-1}$ by taking $D = 1.0 \times 10^{-6}$ cm$^2$ s$^{-1}$ and the hopping length ($l$) as 0.99 nm based on the equation of $k = 6 \times D/l^2$. The value of $l$ is taken to be the average of the shortest site−site distance along the $c$ axis (0.819 nm)[23] and the second shortest site−site distance along the $a$ axis and $b$ axis (1.076 nm)[23].

**1−2. Multiexponential Decay of $[Ru_{0.885}Os_{0.115}(bpy)_3](PF_6)_2$.** The decay of the $^3$CT(Ru) emission at $16.6 \times 10^3$ cm$^{-1}$ from $[Ru_{0.885}Os_{0.115}(bpy)_3](PF_6)_2$ with 11.5% $Os^{2+}$ was observed to decay nonlinearly as shown in part b of Figure 1. The more-rapid initial decay compared to the later stages can be ascribed to the excitation transfer to proximal cations of $[Os(bpy)_3]^{2+}$ in a small number of hops. The possibility of $^3$CT(Ru) triplet−triplet annihilation is excluded because the intensity of the excitation laser was too low to cause it.[8] The bimolecular rate constant of excitation transfer $k_{ent}(t)$, which is a function of time, is expressed by eq 2, provided the lattice of the crystal is isotropic.

$$k_{ent}(t) = 4\pi R_{eff} D\left(1 + \frac{R_{eff}}{\sqrt{\pi D t}}\right) \qquad (2)$$

An attempt to determine the excitation diffusion constant based on the multiexponential decay curve was not made any more because of the ambiguity in the value of $R_{eff}$, some error in the determination of $k_{ent}(t)$, and the poor applicability of eq 2 to the excitation-diffusion in the anisotropic crystals examined.

**2. Step-by-Step Monte Carlo Simulation of Single-Exponential Emission Decays.** A step-by-step Monte Carlo simulation has been applied in the past for the analysis of the decays of photoexcited or radiation-activated species in anisotropic or heterogeneous solids.[7,14−17] In this work, the photoexcitation of $[Ru(bpy)_3]^{2+}$ and the doping of $[Os(bpy)_3]^{2+}$ at a mole fraction of $x$ in the crystal of $[Ru(bpy)_3](X_2)_2$ as well as the deactivation of excited $[Ru(bpy)_3]^{2+}$ were prepared through the generation of random numbers. Both 2500 of the photoexcitation and $x \times 60^3$ of the doped $[Os(bpy)_3]^{2+}$ were distributed among $60^3$ sites, by generating a 3D random number ($n_a$, $n_b$, $n_c$) in the range of 1−60.

The deactivation of excited $[Ru(bpy)_3]^{2+}$ via spontaneous processes and energy transfer to $[Os(bpy)_3]^{2+}$ were taken as they occurred in a time interval $\Delta t$ smaller than 600 ps, when the random number generated in the range between 0 and 1 was lower than the probability of deactivation,

$$\left(\frac{k_{spon} + \sum k_{et}(r)}{k_{spon} + \sum k_{et}(r) + \sum k_{hop}(r)}\right) \times \lfloor 1 - \exp(-(k_{spon} + \sum k_{et}(r) + \sum k_{hop}(r))\Delta t)\rfloor$$

where $k_{spon}$, $k_{et(r)}$, and $k_{hop}(r)$ are the observed rate of spontaneous decay, a presumed rate of excitation transfer to an $[Os(bpy)_3]^{2+}$ at a distance of $r$, and a presumed rate of excitation hopping[26] to neighboring sites at a distance of $r$, respectively. The rates of excitation hopping of the 2500 excited cations to the nearest and the next-nearest sites along the crystal axes via dipole−dipole interaction were calculated in the way shown in the next section, by considering the distances and configurations between the transition dipoles of an excited site and the nearest site. Similarly, the rates of the excitation hopping via super-exchange interaction were calculated (in the next section) by considering the distances and configurations between the bpy ligands of an excited site and the neighboring site. If there were an $[Os(bpy)_3]^{2+}$ at the neighboring sites, the rates of excitation transfer to the nearest and the next-nearest sites along the crystal axes were calculated in the same way. Excitation hopping to the neighboring sites of $[Ru(bpy)_3]^{2+}$ was similarly taken to occur in $\Delta t$ when a random number between 0 and 1 was lower than the probability of hopping, $(\sum k_{hop}(r)/(k_{spon} + \sum k_{et}(r) + \sum k_{hop}(r))) \times [1 - \exp(-(k_{spon} + \sum k_{hop}(r) + \sum k_{et}(r))\Delta t)]$. The time interval of $\Delta t$ was taken to make the sum total of the probabilities of deactivation and of excitation hopping smaller than 1%. The distances between the excited site and neighboring sites were calculated from the coordinates of the sites.

All of the 2500 cations that were excited were examined successively. If the excitation hopping to a neighboring site was evaluated to occur in a time interval $\Delta\tau$, the rate of transfer was recalculated using the distance and the configuration between a newly born excited site and a neighboring site. In the next interval of time, the deactivation and hopping of the surviving excited cations were examined by generating a random number in a step-by-step manner until the number of excited host cations was reduced to four. A time profile of the number of excited sites that survived was obtained, and the numbers of hops to the neighboring sites were

(21) Smoluchowski, *Z. Phys. Chem.* **1918**, *92*, 129.
(22) (a) Harrowfield, J. M.; Sobolev, A. N. *Aust. J. Chem.* **1994**, *47*, 763. (b) Krausz, E.; Riesen, H.; Rae, A. D. *Aust. J. Chem.* **1995**, *48*, 929.
(23) (a) Rillema, D.P.; Jones, D.S. *J. Chem. Soc., Chem. Commun.* **1979**, 849.(b) Biner, M.; Bürgi, H.-B.; Ludi, A.; Röhr, C. *J. Am. Chem. Soc.* **1992**, *114*, 5197.
(24) Dexter, D. L. *J. Chem. Phys.* **1953**, *21*, 836.
(25) Förster, T. *Discuss. Faraday Soc.* **1959**, *33*, 2543.

(26) In the previous step-by-step Monte Carlo simulation,[7] the deactivation and the hopping of the excited state was examined in the order. That is, the deactivation at the first time was examined by comparing the fraction, $[1 - \exp(-(k_{spon} + \sum k_{et})\Delta t)]$, of deactivation with a random number generated. If the excitation was survived, the hopping to the neighboring sites was similarly tested, and the coordinates of the newly born excitation site were reassigned.

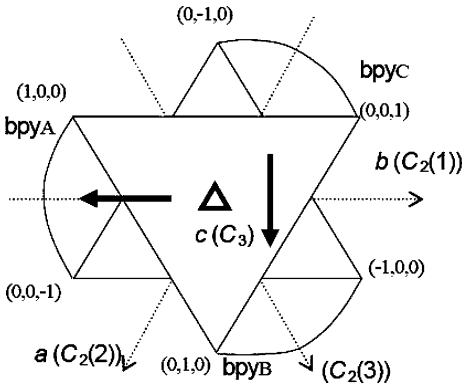


**Figure 2.** Crystal axes of the $PF_6$ salt crystal (*a*, *b*, and *c*), a $C_3$ symmetry axis, and three $C_2$ symmetry axes of the $[M(bpy_A)(bpy_B)(bpy_C)]^{2+}$ (triangle and dotted arrows), Cartesian coordinates of six nitrogen atoms of bpys, and the transition dipoles to the lowest-triplet MLCT state (bold arrows).

calculated. The time profiles of the survived excitation thus prepared were convoluted by the use of an instrumental response function (IRF) for comparison with the observed time profile of emission.

**2−1. Rates of Excitation Hopping via Dipole−Dipole Interaction.** The triplet metal-to-ligand charge-transfer state of $[Ru(bpy)_3]^{2+}$ ($^3$CT(Ru)) has a transition dipole moment ($\mu$) on the base of excitation delocalization through the identical metal−ligand subunits of $[Ru(bpy)_3]^{2+}$ in the crystal around 298 K. For the lowest excited states of $[Ru(bpy)_3](PF_6)_2$ and $[Os(bpy)_3](PF_6)_2$ in the neat crystal at very low temperatures, both the lowest excited state localized on a single metal−ligand subunit and the lowest excited state delocalized through the metal−ligand subunits has been proposed.[5,6,13] Recently, Nozaki et al. demonstrated that the poorly resolved emission spectrum of crystalline $[Ru(bpy)_3](PF_6)_2$ at very low temperatures can be successfully reproduced using a crude adiabatic approximation of vibronic states, and the geometries of the excitation delocalized state can be obtained by density functional theory.[27] Elevation of the temperature, moreover, could enhance delocalization of the excitation through metal−ligand subunits induced by vibronic coupling. The second- and the third-lowest excited spin−orbit states, which are populated around 298 K, have large dipole−dipole interactions between three metal−ligand subunits because of the large transition dipole moments compared to the lowest one.[28,29]

Following to Orgel's notation[30] of the molecular coordinates of $[Ru(bpy)_3]^{2+}$, a symmetry axis of $C_3$ agrees with a diagonal line passing through (1,1,1) and (0,0,0), and three symmetry axes of $C_2$ agree with one of the lines bisecting the molecular plane of $bpy_A$, $bpy_B$, or $bpy_C$, as shown in Figure 2. An excited electron occupies the degenerated LUMO orbitals of $\pi^*_{E+}$ and $\pi^*_{E-}$ composed from the orbitals ($\pi^*_A$, $\pi^*_B$, $\pi^*_C$) of three 2,2′-bipyridines ($bpy_A$, $bpy_B$, $bpy_C$), and a hole occupies the HOMO orbitals composed from the $d_\pi$ orbitals ($d_{xy}$, $d_{yz}$, $d_{zx}$) of Ru(II). The electron excitation

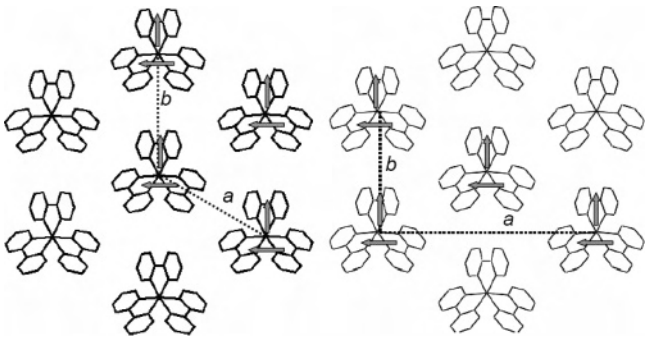


**Figure 3.** Alignment of the dipole moments of the second-closest neighbors relative to the *a* and *b* axes of the $PF_6$ salt crystal [a] on the left-hand, and alignment of the dipole moments of the second- and the third-closest neighbors relative to the *a* and *b* axes of the $ClO_4$ salt crystal [b] on the right-hand. a, ref 23; b, ref 22.

into either $\pi^*_{E+}$ or $\pi^*_{E-}$ shown in the following equations is involved in the metal-to-ligand charge transfer (MLCT) transition,

$$\pi^*_{E+} = (2\pi_A - \pi_B - \pi_C)/\sqrt{6} \quad (3)$$

$$\pi^*_{E-} = (\pi_B - \pi_C)/\sqrt{2} \quad (4)$$

The transition dipole moment can be expressed by using a direction ($\mu/|\mu|$) and a magnitude (either $\epsilon_{ab}(\bar{\nu})/\bar{\nu}$ or $1/(\tau_0\bar{\nu}^3)$) of a transition dipole ($\mu$) at wave numbers ($\bar{\nu}$), where $\epsilon_{ab}(\bar{\nu})$ and $\tau_o$ are the optical absorption coefficient and the radiative lifetime of the excited state, respectively.

As Figure 2 shows, a transition dipole shown in an arrow, $\mu_+$, lies along one of three $C_2$ axes of the $[Ru(bpy)_3]^{2+}$, $C_2(1)$, and the other dipole, $\mu_-$, is perpendicular to $\mu_+$. The magnitude of the dipoles, $\mu_+$ and $\mu_-$, are $^1/_2$ of a unit dipole moment. Every dipole moment of the $\mu_+$ and $\mu_-$ of the cations is uniquely set in the $ClO_4^-$ salt crystal as the $C_3$ axis, and one of the $C_2$ axes of $[Ru(bpy)_3]^{2+}$ is nearly parallel to the *c* axis and the *b* axis of the $ClO_4^-$ salt crystal, respectively. That is, the $\mu_+$ and the $\mu_-$ of the cations in the $ClO_4^-$ salt crystal are aligned along the *b* and the *a* axes, respectively. As for the hexagonal crystal of the $PF_6^-$ salt shown in Figure 3, the $\mu_+$ of the cations is parallel to the *b* axis, too.

The rates of excitation hopping due to dipole−dipole interactions $k_{hop(d-d)}(r)$ are calculated by using the following equations,

$$k_{hop(d-d)}(r) = \frac{9000 \ln 10}{128\pi^5 N n^4} V^2 I(\bar{\nu}) \quad (5)$$

$$I(\bar{\nu}) = \frac{1}{\tau_0}\int f_{em}(\bar{n})\epsilon_{ab}(\bar{\nu})\frac{d\bar{\nu}}{\bar{\nu}^4} \quad (6)$$

$$V = V_{++} + V_{+-} + V_{-+} + V_{--} \quad (7)$$

where $V^2 \times I(\bar{\nu})$ is the dipole−dipole interaction energy between the absorption of an acceptor and the emission of a donor under resonance conditions. $V^2$ is a configuration factor between cations, which is defined as the square of the interaction energy $V$ between the unit dipoles of a donor and an acceptor. Each of the dipole−dipole interactions

(27) Nozaki, K.; Takamori, K.; Nakatugawa, Y.; Ohno, T. *Inorg. Chem.* **2006**, *45*, 6161.
(28) Harrigan, R. H.; Crosby, G. A. *J. Chem. Phys.* **1973**, *59*, 3468.
(29) Hager, G. D.; Crosby, G. A. *J. Am. Chem. Soc.* **1975**, *97*, 7031.
(30) Orgel, L. E. *J. Chem. Soc.* **1961**, 3683.

**Table 2.** Distance and Coordinates of Neighboring Sites and Numbers of the Equivalent Sites in the Crystals of $[Ru(bpy)_3]X_2$

| crystal | site−site distance nm | change in a unit of the length of *a* axis | change in a unit of the length of *b* axis | change in a unit of the length of *c* axis | number of equivalent sites, *n* |
|---|---|---|---|---|---|
| $[Ru(bpy)_3](PF_6)_2$[a] | 0.819 | 0 | 0 | ±0.5 | 2 |
| | 1.076 | 0 | ±1 | 0 | 2 |
| | 1.076 | ±1 | 0 | 0 | 2 |
| | 1.076 | ±1 | ±1 | 0 | 2 |
| | 1.352 | 0 | ±1 | ±0.5 | 4 |
| | 1.352 | ±1 | 0 | ±0.5 | 4 |
| | 1.352 | ±1 | 0 | ±0.5 | 4 |
| $[Ru(bpy)_3](ClO_4)_2$[b] | 0.797 | 0 | 0.0418 | ±0.5 | 2 |
| | 1.033 | ±0.5 | ∓0.5 | 0 | 2 |
| | 1.033 | ±0.5 | ±0.5 | 0 | 2 |
| | 1.076 | 0 | ±1 | 0 | 2 |
| | 1.279 | ±0.5 | 0.4582 | ±0.5 | 2 |
| | 1.294 | ±0.5 | 0.4582 | ±0.5 | 2 |
| | 1.303 | 0 | 0.9582 | ±0.5 | 2 |
| | 1.316 | ±0.5 | −0.5418 | ±0.5 | 2 |
| | 1.330 | ±0.5 | −0.0542 | ±0.5 | 2 |

[a] Ref 23. [b] Ref 22.

between the cations consists of four interaction energies, one of which is written in the following equation for the unit dipoles, $\mu_+$ and $\mu_+'$, of donor and acceptor, respectively

$$V_{++} = \left(\frac{1}{\sqrt{2}}\right)^2 \frac{(\mu_+)(\mu_+') - 3((\mu_+)(\vec{R}_{++}/R_{++}))((\mu_+')(\vec{R}_{++}/R_{++}))}{R_{++}^{\ 3}} \quad (8)$$

where $R_{++}$ and $\vec{R}_{++}$ are a distance and a distance vector between the centers of unit dipoles, $\mu_+$ and $\mu_+'$, respectively. It is necessary to know the angle $\theta_{++}$ between the unit dipoles of a donor $\mu_+/|\mu_+|$ and an acceptor $\mu_+'/|\mu_+'|$ for the evaluation of the first term of eq 8. The angle $\theta_{++}$ is evaluated from the following equation, $\cos(\theta_{++}) = l_+l_+' + m_+m_+'_+ n_+n_+'$, where $l_+$, $m_+$, $n_+$ are the *x*, y, and *z* projections of the unit vector pointing to the center of $bpy_A$ of the donor, respectively, and $l_+'$, $m_+'$, $n_+'$ are the *x*, *y*, and z projections of the unit vector directing to the center of $bpy_A'$ of the acceptor, respectively. It is also necessary to know the cosine between the dipole and the dipole−dipole distance vector for the evaluation of the second term of eq 8. The corresponding angles were calculated in a similar way from the projections of the dipole and distance vectors. The projections of a dipole vector and a distance vector were estimated from the coordinates and length of the dipole and distance vectors based on the crystallographic data of $[Ru(bpy)_3]X_2$.[7,22,23] The hopping distances were calculated from the coordinates of the close sites along the unit cell axes (*a*, *b*, *c*). The directions of short-length excitation hopping were obtained from the crystallographic data of $[Ru(bpy)_3]X_2$, as shown in Table 2.

$I(\bar{\nu})$ is a product of an integral and the radiative lifetime ($\tau_o$) of $[Ru(bpy)_3]^{2+}$, as eq 6 shows. The extent of the integral is estimated to be $4.2 \times 10^{-14}$ for the excitation transfer to $[Os(bpy)_3]X_2$ and $0.24 \times 10^{-14}$ $mol^{-1}cm^6$ for the excitation hopping to $[Ru(bpy)_3]X_2$ from the donor emission spectrum and the acceptor absorption spectrum, respectively. The radiative lifetime of $[Ru(bpy)_3]^{2+}$ at 298 K is calculated to be 15 $\mu$s by using a relation, $\Phi = \tau/\tau_o$, from the quantum yield ($\Phi = 0.042$) and the lifetime ($\tau = 0.63$ $\mu$s) of the donor emission in $H_2O$.[31] The radiative lifetime of $[Ru(bpy)_3]^{2+}$ was almost independent of solvents (water, dichloromethane, pyridine, *N*,*N*′-dimethylformamide, acetonitrile, and so on), in which the emission yields (0.063 in acetonitrile, for instance) referred to that in water.[32] A distorted molecular structure of $[Ru(bpy)_3]^{2+}$ on the charge-transfer excitation in the polar solvents could, however, tune the radiative lifetime in the crystal to some extent.[27] Moreover, there are a few indications that the radiative lifetime of $[Ru(bpy)_3]^{2+}$ at 298 K is shorter than 10 $\mu$s. A radiative lifetime of 9.5 $\mu$s in acetonitrile can be estimated from a relatively large yield (0.090), which referred to that of 9,10-diphenylanthracene.[33] Another radiative lifetime (6.5 $\mu$s) at 298 K can be derived from the quantum yield ($\Phi = 0.2$) and the lifetime ($\tau = 1.3\mu$s) of the $PF_6^-$ salt crystal ground with MgO.[34] A short radiative lifetime of 7.8 $\mu$s in non-reorientating media at 298 K is estimated in a different way. Harrigan and Crosby derived the radiative rates ($k_{1r}$, $k_{2r}$, $k_{3r}$) and the energy levels ($\epsilon_1$, $\epsilon_2$, $\epsilon_3$) of the three closely lying states of $[Ru(bpy)_3]^{2+}$ in polymethylmethacrylate on the basis of the temperature-dependent yield and the radiative rate in a temperature range of 4−77 K.[29] Assuming that only the populations of the three states are dependent on the temperature in a temperature range of 77−298 K, a radiative lifetime is calculated to be 7.8 $\mu$s, by inserting the radiative rates ($k_{1r}$, $k_{2r}$, $k_{3r}$) and the energy levels($\epsilon_1$,$\epsilon_2$,$\epsilon_3$) of the three closely lying lowest states into a formula of the temperature-dependent radiative rates.[35] Because there is a close resemblance between the three, an effect of the radiative lifetime (7.8 $\mu$s) on the simulation of the emission decay will be examined, too.

In the previous work,[7] the extent of the dipole−dipole interaction between a donor and an acceptor was calculated in an oversimplified way; the dipole moment of the complex cation was put in the center of the cation with a random

(31) Van Houten, J.; Watts, R. J. *J. Am. Chem. Soc.* **1976**, *98*, 4853.
(32) Casper, J.V.; Meyer, T. J.; *J. Am. Chem. Soc.* **1983**, *105*, 5583.
(33) Abedin-Siddique, Z.; Ohno, T.; Nozaki, K.; Tsubomura, T. *Inorg. Chem.* **2004**, *43*, 663.
(34) Islam, A. *Thesis*, Osaka University 1998.
(35) $k_r(T) = (k_{1r} + 2k_{2r}\exp(-(\epsilon_2 - \epsilon_1)/kT) + k_{3r}\exp(-(\epsilon_3 - \epsilon_1)/kT))/(1 + 2\exp(-(\epsilon_2 - \epsilon_1)/kT) + \exp(-(\epsilon_3 - \epsilon_1)/kT))$, which is in ref 29.

**Table 3.** Crystal Structures, Site−Site Distances ($R$), Configuration Factors of Dipole−Dipole Interaction ($V^2$) between Neighboring Cations in the $[Ru(bpy)_3]X_2$ Crystals and Hopping Rates of $k_{hop(d-d)}(r)/10^6$ $s^{-1}$ via Dipole−Dipole Interaction, the Shortest Pyridyl−Pyridyl Distance $r_{ikjl}$ between Neighboring Cations and Hopping Rates of $k_{hop(ex)}(r)/10^6$ $s^{-1}$ via Exchange Interaction

| crystals, space group, an angle ($\neq 90$) between axes, and number of sites in the unit cell ($Z$) | $R$/nm (axis)[a] | $1/R^6$ $\times 10^{-40}$ $cm^{-6}$ | $V^2$ $\times 10^{-40}$ $cm^{-6}$ | $V^2/(1/R^6)$ | $k_{hop(d-d)}(r)$ $\times 10^{-6}$ $s^{-1}$ | shortest $r_{ikjl}$/nm | $k_{hop(ex)}(r)$ $\times 10^{-6}$ $s^{-1}$ |
|---|---|---|---|---|---|---|---|
| $[Ru(bpy)_3](ClO_4)_2$, | 0.797($c$) | 391 | 180 | 0.46 | 51 | 0.54 | 720 |
| $C2/c$, $\beta$=90.76, | 1.033 | 84.2 | 210 | 2.5 | 58 | 0.55 | 860 |
| and $Z=4$[b] | 1.033 | 84.2 | 34 | 0.40 | 9.3 | 0.55 | 860 |
| | 1.076($b$) | 64.4 | 17 | 0.26 | 4.7 | 0.57 | 930 |
| | 1.279 | 22.8 | 33 | 1.45 | 9.2 | 0.80 | 59 |
| | 1.294 | 21.3 | 4 | 0.19 | 1.1 | 0.80 | 59 |
| | 1.316 | 19.3 | 4.2 | 0.22 | 1.2 | 0.80 | 59 |
| | 1.330 | 18.0 | 31 | 1.74 | 8.7 | 0.80 | 59 |
| $[Ru(bpy)_3](PF_6)_2$, | 0.819($c$) | 331 | 194 | 0.59 | 54 | 0.58 | 305 |
| $P-3c1$, $\gamma$=120, | 1.076($a$) | 64.4 | 175 | 2.71 | 48 | 0.58 | 756 |
| and $Z=2$[c] | 1.076($b$) | 64.4 | 15.6 | 0.24 | 4.3 | 0.58 | 756 |
| | 1.076 | 64.4 | 30.3 | 0.47 | 8.4 | 0.58 | 756 |
| | 1.352 | 16.5 | 16.8 | 1.02 | 4.7 | 0.76 | 7.8 |
| | 1.352 | 16.5 | 7.3 | 0.59 | 2.7 | 0.76 | 7.8 |
| | 1.352 | 16.5 | 1.8 | 0.11 | 0.51 | 0.76 | 7.8 |
| $[Ru(bpy)_3](SbF_6)_2$, | 0.863($c$) | 242 | 183 | 0.61 | 50 | 0.61 | 160 |
| $P-3c1$, $\gamma$=120, | 1.080($a$) | 62 | 132 | 2.12 | 37 | 0.58 | 696 |
| and $Z=2$[d] | 1.080($b$) | 62 | 16 | 0.26 | 4.4 | 0.58 | 696 |
| | 1.383 | 14.3 | 14 | 0.99 | 3.3 | 0.77 | 4.2 |
| | 1.383 | 14.3 | 6 | 0.42 | 1.5 | 0.77 | 4.2 |

[a] An axis is shown in parenthesis in the case where sites are put along the crystal axis. [b] Ref 22. [c] Ref 23. [d] This work.

orientation. The extent of dipole−dipole interaction was taken to be dependent on the metal−metal distance only.[7]

**2−2 Rates of Excitation Hopping Between Neighboring Cations via Dipole−Dipole Interaction Mechanism.** An interaction energy between unit dipoles of a donor and an acceptor was calculated to be $\pm 2/R^3$ in the case where the dipoles of a donor and an acceptor are collinear (i.e., head-to-tail or head-to-head arrangements), so that the value of the second term of eq 8 is three. If the dipoles of the donor are parallel to those of the acceptor and perpendicular to the distance vector so that the second term of eq 8 goes to zero, meanwhile, an interaction energy between unit dipoles is reduced to $\pm(1/R^3)$. The square of configuration factors $V^2$ between the dipoles mentioned above are the squares of the interaction energy, $(\pm 2/R^3)^2$ and $(\pm 1/R^3)$,[2] respectively.

The configuration factors $V^2$ between neighboring cations at various distances in the crystals are calculated on the basis of eqs 7 and 8. To look at the total effect of the configuration between the cations separated by a distance of $R$ on $V^2$, those quantities are compared in Table 3 with that of $(1/R^6)$ between parallel dipoles at the metal centers of a donor and an acceptor. The ratios of $V^2/(1/R^6)$ are as small as 1:2 for the closest neighbors in the $PF_6^-$ salt and the $ClO_4^-$ salt crystals. Meanwhile, the ratios of $V^2/(1/R^6)$ are much less than unity for the second-closest neighbors, except for those put on the $a$ axis in the $PF_6^-$ salt crystal and those put halfway between the $a$ and the $b$ axes in the $ClO_4^-$ crystal.

On the basis of the rates of excitation hopping to $[Ru(bpy)_3]^{2+}$ and excitation transfer to $[Os(bpy)_3]^{2+}$ at the neighboring sites listed in Table 3 and spontaneous decay, a step-by-step Monte Carlo simulation gave rise to a time profile of emission intensity shown in the solid lines in Figure 1. All of the decays of emission simulated on the basis of the dipole−dipole interaction mechanism are slower than those observed. The slopes of the calculated curves are less than 30% of those observed. Whereas fast decay profiles of the Ru(II) emission (the broken lines in Figure 1) were simulated using the calculated radiative life (7.8 $\mu$s) at 298 K, the rates of excitation hopping and excitation transfer due to the dipole−dipole interaction mechanism are insufficient for the emission decay observed. A short-distance exchange interaction mechanism of excitation hopping seems to be indispensable as well as a long-distance dipole−dipole interaction mechanism, because there are sites with a shorter distance than 1.1 nm for those crystals.

**2−3 Excitation Hopping in $[Ru_{1-x}Os_x(bpy)_3](PF_6)_2$ ($x \leq 0.01$) via Dipole−Dipole and Exchange Interactions.** The magnitude of exchange interactions between the cations in the triplet excited state and the ground state may be complexly dependent upon the configuration between 3D $\pi$ orbitals of neighboring cations at different distant sites compared with interactions between 1D transition dipoles. Instead of performing elaborate quantum chemical calculations of the exchange interactions, the time profiles of emission were simulated by adapting the rates of excitation hopping to the host cations and excitation transfer to the guest cations via the exchange mechanism as adjustable parameters in a step-by-step Monte Carlo simulation. More than two adjustable parameters, which characterize the rates of both the hopping to the host cations and the transfer to the guest cations at nearly neighboring sites, are necessary for simulation of the emission decay profiles. However, each parameter of them brings about increased chances of the system falling into local minima of simulation. It is crucial to diminish the number of variable parameters for the sake of reliable simulation.

Exchange interactions of both electron and hole between a donor and an acceptor are necessary to induce both excitation transfer and excitation hopping. The rates of the transfer and hopping are dependent on the magnitude of the hole-exchange interaction in as much as a hole is in the first approximation localized at the metal centers of the cations, causing the magnitude of the hole-exchange interaction to be much smaller than that of the electron-exchange interaction. A hole of an MLCT state has a super-exchange interaction through the $\pi$ orbitals of the 2,2′-bipyridines with the neighboring cations that is more favorable than the direct-exchange interaction between d$\pi$ orbitals at the metal centers; a DFT calculation[36] showed that a hole of an MLCT state is extended into the $\pi$ orbitals of 2,2′-bipyridines ($e_1$) with a density of 20%. Overlap of the d$\pi$ orbitals of Ru(II) with the $\pi$ orbitals of 2,2′-bipyridines of cations, therefore, play the most important role in the hole-exchange interaction. In addition, a DFT calculation[36] revealed that the overlap of Ru(II) d$\pi$ orbitals with the lowest $\pi$* orbitals of 2,2′-bipyridines of cations ($a_2$) is negligibly small. The magnitude of the exchange interaction, $K$, might be a function of the center−center distance, $r_{ikjl}$, and the plane−plane configuration between pyridyl moieties of the $i$-th 2,2′-bipyridine of a donor ($i$ = A, B, C) and the $j$-th 2,2′-bipyridine of an acceptor ($j$ = A′, B′, C′). The interacting moieties would be the $k$-th pyridyl group of $i$-th 2,2′-bipyridine of the donor and the $l$-th pyridyl group of $j$-th 2,2′-bipyridine of the acceptor ($k$ = 1 and 2, and $l$ = 1 and 2). As an approximation, $K_{ij}$ can be written by using a van der Waals distance $r_o$ between centers of the pyridyl moieties and the distance-attenuation factor ($\beta$) of six $\pi$ orbitals of the pyridyl moieties in the following equation,

$$K_{i,j} = \frac{\alpha}{6}\sum_{l}^{2}\sum_{k}^{2}\exp(-\beta(r_{ikjl} - r_0)) \qquad (9)$$

where $\alpha/6$ is the density of the $\pi$ orbital of each pyridyl moiety in the HOMO mainly composed from the d$\pi$ orbitals. The $\pi$ orbitals outside the sphere with a radius of van der Waals distance ($r_o$) are proportional to the distance in this model.

The van der Waals distance (0.42 nm) between pyridyl moieties of neighboring molecules $r_o$ was taken as an intermediate between the shortest pyridyl−pyridyl distances of the face-to-face (0.36 nm) and the face-to-edge approaches (0.47 nm) of the pyridyl moieties, which is a little shorter than the pyridyl−pyridyl distance between the bpy ligands in $[Ru(bpy)_3]^{2+}$ (0.50 nm).[23] The shortest center−center distances between pyridyl moieties of neighboring cations $r_{ijkl}$ are very similar (0.58 nm) for the nearest and the next-nearest neighbors in the $PF_6^-$ salt crystal and are 0.54 and 0.55 nm, respectively, for the $ClO_4^-$ salt crystal, although the metal−metal distance between the nearest neighbors is shorter than that of the next-nearest ones by 0.25 nm. The $C_3$-axes of the cations are collinear for the nearest neighbors, whereas the $C_2$ axes of the cations are collinear for the next-nearest neighbors. The difference in the intermolecular configuration between the nearest neighbors and the next-nearest neighbors is responsible for the similarly short pyridyl−pyridyl distances.

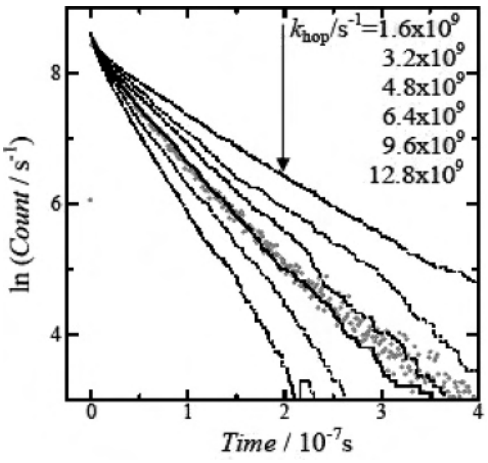


**Figure 4.** Effect of $k^0_{hop}$ on the simulated emission decay of $[Ru_{0.99}Os_{0.0099}](bpy)_3](PF_6)_2$ with $k^0_{hop}/10^9$ s$^{-1}$ shown, a $k^0_{et}$ of 3.2 × 10$^{11}$ s$^{-1}$, and a $\beta$ of 1.0 nm$^{-1}$.

A Monte Carlo simulation of emission decay was made by adopting three adjustable parameters: a common distance-attenuation factor of both the hopping and the transfer rates, $\beta$, a limiting rate of the hopping to an imaginary $[Ru(bpy)_3]^{2+}$ at the van der Waals distance, $k^0_{hop}$, and a limiting rate of the transfer to an imaginary $[Os(bpy)_3]^{2+}$ at the van der Waals distance, $k^0_{et}$. In other words, the rates of excitation hopping to a host ion at a distance of $r_{ikjl}$, $k_{hop}$, and excitation transfer to a guest at a distance of $r_{ikjl}$, $k_{et}$, are expressed in the following equations,

$$k_{hop} = k^0_{hop}\sum_{i}^{3}\sum_{j}^{3}K_{i,j}^{\ 2} = k^0_{hop}\,\alpha^2\sum_{i}^{3}\sum_{j}^{3}\sum_{k}^{2}\sum_{l}^{2}\frac{1}{36}\exp(-2\beta(r_{ikjl} - r_o)) \qquad (10)$$

$$k_{et} = k^0_{et}\sum_{i}^{3}\sum_{j}^{3}K_{i,j}^{\ 2} = k^0_{et}\,\alpha^2\sum_{i}^{3}\sum_{j}^{3}\sum_{k}^{2}\sum_{l}^{2}\frac{1}{36}\exp(-2\beta(r_{ikjl} - r_o)) \qquad (11)$$

where $k^0_{hop}$ and $k^0_{et}$ can be expressed in terms of the Franck−Condon weighted density and the electronic interaction energy of excitation hopping and excitation transfer, respectively, assuming that the process is nonadiabatic. The products, $k^0_{hop} \times \alpha^2$ and $k^0_{et} \times \alpha^2$, are rewritten as $k^0_{hop}$ and $k^0_{et}$, respectively, for convenience hereafter. The simulations of the emission decays were performed by tuning the effective rates of excitation hopping to the host ions at the close sites and excitation transfer to the guest ions at the close sites via the exchange and dipole−dipole mechanisms. The parameters, $\beta$ in a small range of (7−13) nm$^{-1}$ and $k^0_{hop}$ in a small range of (1.6−12.8) × 10$^9$ s$^{-1}$ with the van der Waals distance of 4.2 nm, varied the decay profiles a lot, as shown in Figures 4 and 5. Both $\beta$ and $k^0_{hop}$ are not uniquely

(36) Daul, C.; Baerends, E. J.; Vernooijs, P. *Inorg. Chem.* **1994**, *33*, 3538.

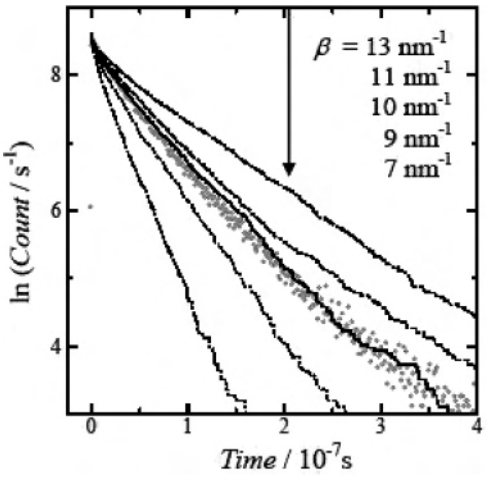


**Figure 5.** Effect of $\beta$ on the simulated emission decay of $[Ru_{0.99}Os_{0.0099}](bpy)_3](PF_6)_2$ with a $\beta$ of 1.0 $nm^{-1}$ shown, a $k_{hop}^0$ of $0.64 \times 10^{10}$ $s^{-1}$, and a $k_{et}^0$ of $3.2 \times 10^{11}$ $s^{-1}$.

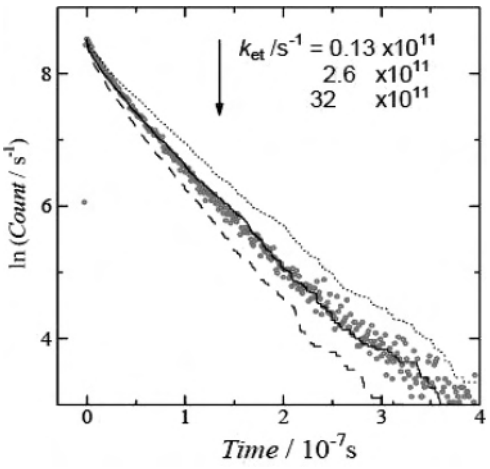


**Figure 6.** Effect of $k_{et}^0$ on the simulated emission decay of $[Ru_{0.9901}Os_{0.0099}](bpy)_3](PF_6)_2$ with $k_{et}^0/10^{10}s^{-1}$ shown, a $k_{hop}^0$ of $0.64 \times 10^{10}$ $s^{-1}$, and a $\beta$ of 10 $nm^{-1}$.

determined because neither $\beta$ nor $k_{hop}^0$ is an independent variable. The value of $\beta$ was taken as 10 $nm^{-1}$ tentatively; the other adjustable parameter of $k_{hop}^0$ in the simulation was thus uniquely determined to be $0.64 \times 10^{10}$ $s^{-1}$. This method for the tentative dertermination of $k_{hop}^0$ was applied to the emission decay of the more-concentrated crystals of $[Ru_{0.94}Os_{0.06}(bpy)_3](PF_6)_2$ and $[Ru_{0.885}Os_{0.115}(bpy)_3](PF_6)_2$. The value of $k_{hop}^0$ was determined to be $0.64 \times 10^{10}$ and $1.15 \times 10^{10}$ $s^{-1}$ under the same presumption of $\beta = 10$ $nm^{-1}$ although the simulated decays of emission are strongly dependent on both $k_{hop}^0$ and $k_{et}^0$. The mean of the three limiting rate-constants of hopping is $0.83 \times 10^{10}$ $s^{-1}$, which will be utilized to estimate the value of $\beta$ for the other crystals of $ClO_4^-$ and $SbF_6^-$ salts on reference to the $PF_6^-$ salt crystal. The extent of $k_{et}^0$ ($\approx 3 \times 10^{11}$ $s^{-1}$) will be more accurately determined in section 3. By using another radiative lifetime of $[Ru(bpy)_3]^{2+}$ (7.8 $\mu$s) in the simulation of emission decay profiles, it was determined that the limiting rate constants of excitation hopping to $[Ru(bpy)_3]^{2+}$ and excitation transfer to $[Os(bpy)_3]^{2+}$ at the van der Waals distance are $0.36 \times 10^{10}$ and $1.9 \times 10^{11}$ $s^{-1}$, respectively.

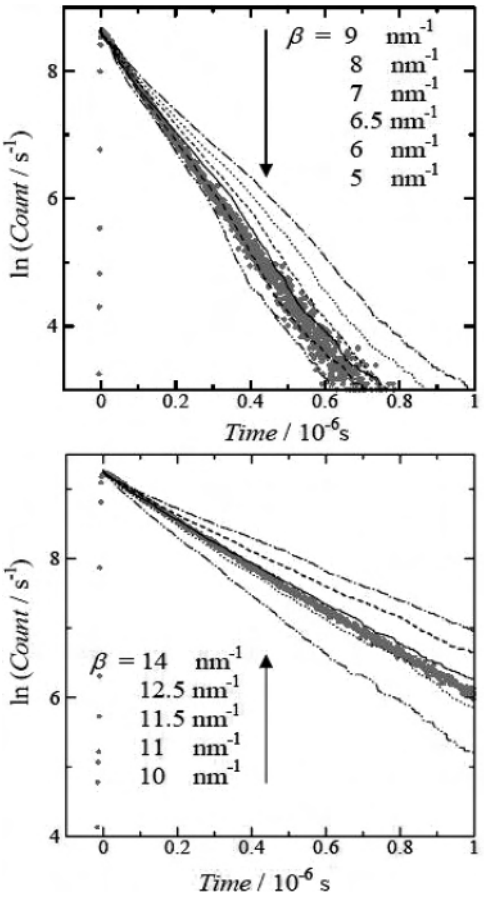


**Figure 7.** Simulated emission decays of $[Ru_{0.995}Os_{0.005}(bpy)_3]$ $(ClO_4)_2$ (above) and $[Ru_{0.997}Os_{0.003}(bpy)_3](SbF_6)_2$ (below). The values of $\beta$ are shown, and those of the other parameters are $k_{et}^0 = 2.6 \times 10^{11}$ $s^{-1}$, and $k_{hop}^0 = 0.83 \times 10^{10}$ $s^{-1}$.

With the use of the values of $k_{hop}^0$ and $\beta$, the rate constants of excitation hopping to the nearest site at 8.19 nm ($k_{hop(ex)}^{first}$) and the next-nearest site at 1.076 nm ($k_{hop(ex)}^{second}$) via exchange interactions of electron and hole were evaluated to be on the order of $10^8$ $s^{-1}$, as shown in Table 6. A similar value of the $k_{hop(ex)}^{second}$ to that of the $k_{hop(ex)}^{first}$ comes from the same value of the smallest pyridyl−pyridyl distance between the nearest neighbors and the next-nearest neighbors. Meanwhile, the form of the cation was assumed to be spherical with a van der Waals distance of 0.6 nm in the previous work[7] so that the rate of hopping due to the exchange interaction between the next-nearest neighbors was thought to be slower than that of the hopping between the nearest neighbors. The rates of hopping to the two nearest sites and the six next-nearest sites via both dipole−dipole and exchange interactions were calculated to be $0.72 \times 10^9$ and $5.4 \times 10^9$ $s^{-1}$, respectively. The total rate of excitation hopping to the nearest and the next-nearest sites ($6.1 \times 10^9$ $s^{-1}$) is reasonably smaller than the rate ($10^{11}$ $s^{-1}$) of excitation hopping to $Pd^{2+}$ at the nearest (0.506 nm) site in the anisotropic crystal of Pd(6-phenyl-bpy)Cl.[5] Moreover, the total rate is 380 times the disappearance rate of a higher-energy site ($1.6 \times 10^7$ $s^{-1}$) because of excitation hopping to the lowest energy site at a distance of 0.916 nm in $[Ru(bpy)_3](PF_6)_2$ at 1.3 K.[5] A large difference in the hopping rate between 298 and 1.3 K may be caused by three possible

**Table 4.** Rates of Excitation Hopping to the Nearest Site ($k_{hop(ex)}^{first}$ and $k_{hop(d-d)}^{first}$) and the Next-Nearest Site ($k_{hop(ex)}^{second}$ and $k_{hop(d-d)}^{second}$) in the $PF_6^-$ Crystal via Exchange and Dipole−Dipole Mechanisms

| | $k_{hop(ex)}^{first}/10^7 s^{-1}$ | $k_{hop(ex)}^{second}/10^7 s^{-1}$ | $k_{hop(d-d)}^{first}/10^7 s^{-1}$ | $k_{hop(d-d)}^{second}/10^7 s^{-1}$ |
|---|---|---|---|---|
| this work | 31 | 76 | 5.4 | 2.0 |
| Tsushima et al.[a] | 36 | 1.8 | (6.1) | (1.2) |

[a] Ref 7.

**Table 5.** Distance-Attenuation Factor $\beta$ for Exchange Mechanism of Excitation Hopping with the Limiting Rate-Constants of $k_{hop}^0$ ($0.83 \times 10^{10}$ $s^{-1}$) and $k_{et}^0$ ($2.6 \times 10^{11}$ $s^{-1}$)

| anion | $PF_6^-$ | $ClO_4^-$ | $SbF_6^-$ |
|---|---|---|---|
| $\beta$ (nm) | 10 | 6.5<br>(7.0)[a] | 11.5<br>(12)[a] |

[a] With another set of limiting Rates, $k_{hop}^0$ ($0.36 \times 10^{10}$ $s^{-1}$) and $k_{et}^0$ ($1.9 \times 10^{11}$ $s^{-1}$).

**Table 6.** Diffusion Constants of Excitation Migration, $D/10^{-6}$ $cm^2$ $s^{-1}$ in the Crystals of $[Ru(bpy)_3]X_2$.

| X | *a* axis | *b* axis | *c* axis |
|---|---|---|---|
| $PF_6^-$ | 9.3 | 9.1 | 1.4 |
| $ClO_4^-$ | 7.2 | 8.3 | 2.6 |

reasons. (1) the second-lowest and the third-lowest spin−orbit MLCT states, which have a larger dipole than the lowest spin−orbit state does, are thermally populated and exhibit more dipole−dipole interactions at a high temperature, (2) the hopping process exhibits some temperature dependence of the rate due to a potential barrier of 400 $cm^{-1}$, which is inferred from the sum of the vibrational reorganization energies (≈800 $cm^{-1}$) of the lowest-triplet MLCT,[27] and (3) the barrier height of hopping is higher at 1.3 K because the symmetry reduction in the space group of the crystal below 105 K[20b] raises the barrier height. A study of the effect of the temperature on the hopping rate is now in progress to investigate the two possible mechanisms of tunneling and barrier crossing.

**2−4 Excitation Hopping of $[Ru_{1-x}Os_x(bpy)_3](X)_2$ (X = $ClO_4^-$ and $SbF_6^-$, $x \leq 0.01$) via Dipole−Dipole Interaction and Exchange Interaction.** The intermolecular configuration between an excited cation and the nearest or the third-nearest one in the $ClO_4^-$ salt crystal is very similar to that between an excited cation and the nearest or the second-nearest one in the $PF_6^-$ salt crystal, although the space group of the former ($C2$)[22] is different from the latter ($P3$).[23] The $C_3$ axis of the cations is collinear to the *c* axis of the lattice, and all of the dipole moments of the cations lie on the *ab* plane for both of the crystals. All of the structural data, distances between dipoles, cosines between dipoles, cosines between a dipole and a distance vector connecting dipoles, and center−center distances between pyridyl moieties of cations were calculated from the coordinates of the carbon, nitrogen, and ruthenium atoms of $[Ru(bpy)_3](ClO_4)_2$.[22] Rates of excitation transfer to the nearest, the second, and the third-nearest sites via dipole−dipole interactions were calculated on the basis of the structural data. All of the structural data for the chloride crystals[8] are available for the calculation of dipole−dipole interactions and for the estimation of the exchange interactions of electron and hole, as a function of the distances between the centers of the pyridyl moieties of neighboring cations, as provided by crystallographic data.

In the step-by-step Monte Carlo simulation, the limiting rates of excitation hopping ($k_{hop}^0$) and excitation transfer ($k_{et}^0$) were taken to be the same as those in the $PF_6^-$ crystal ($0.83 \times 10^{10}$ and $2.6 \times 10^{11}$ $s^{-1}$, respectively). However, the distance-attenuation factor of the exchange interaction $\beta$ may be varied as a result of the various anions lying near the cations in the crystals. Because variations in the dielectric constant, electron polarization, electroconductivity, and of electron donor and acceptor character as a function of the various anions are unknown, $\beta$ was chosen to be an adjustable simulation parameter. The emission decays thus simulated are dependent on two parameters, $\beta$ and $k_{hop}^0$, as in the case of the $PF_6^-$ salt crystal, because the rates of excitation hopping to arbitrary sites are a function of both. With a set of the limiting rates, $k_{hop}^0$ ($0.83 \times 10^{10}$ $s^{-1}$) and $k_{et}^0$ ($2.6 \times 10^{11}$ $s^{-1}$), the variable parameter of distance-attenuation factor $\beta$ in the simulation was optimized to be 6.5 $nm^{-1}$ for the $ClO_4^-$ salt crystal with $Os^{2+}$ at mole fractions of 0.005 (Figure 7) and 0.010. With another set of the limiting rates, $k_{hop}^0$ ($0.36 \times 10^{10}$ $s^{-1}$) and $k_{et}^0$ ($1.9 \times 10^{11}$ $s^{-1}$), on the basis of another radiative rate of $[Ru(bpy)_3]^{2+}$, the variable parameter of distance-attenuation factor $\beta$ in the simulation was optimized to be 7.0 $nm^{-1}$ for the $ClO_4^-$ salt crystal with $Os^{2+}$ at mole fractions of 0.005.

Intermolecular configurations in the $SbF_6^-$ salt crystal were derived from that of the $PF_6^-$ salt crystal because the crystal structure of $[Ru(bpy)_3](SbF_6)_2$ was verified to be isomorphous in the space group $P3c1$ with the $PF_6$ salt by checking the Raue reflections. The only lattice constants were dertermined to be $a = b = 1.080(3)$ and $c = 0.8633(7)$ nm, $\alpha = \beta = 90°$, $\gamma = 120°$, and $Z = 2$. The rates of excitation hopping and excitation transfer via dipole−dipole interactions were calculated from distances between dipoles, cosines between the dipoles, and cosines between the dipole and the distance vector in the $SbF_6^-$ salt crystal by assuming the same molecular structure of the cation as that in the $PF_6^-$ salt crystal. The emission decay of the $SbF_6^-$ crystal containing $Os^{2+}$ at a mole fraction 0.003 was simulated using the rates of the limiting excitation transfer $k_{et}^0$ and hopping $k_{hop}^0$, as determined for the $PF_6^-$ crystal (Figure 7). The optimum simulation gave rise to the magnitude of $\beta$ (11.5 $nm^{-1}$). With other limiting rates, $k_{hop}^0$ ($0.36 \times 10^{10}$ $s^{-1}$) and $k_{et}^0$ ($1.9 \times 10^{11}$ $s^{-1}$), the variable parameter of distance-attenuation factor $\beta$ in the simulation was optimized to be 12 $nm^{-1}$ for the $SbF_6^-$ salt crystal, with $Os^{2+}$ at a mole fraction of 0.003.

**3. Step-by-Step Monte Carlo Simulation of Multiexponential Emission Decays of $[Ru_{0.94}Os_{x0.06}(bpy)_3](PF_6)_2$ and $[Ru_{0.885}Os_{x0.115}(bpy)_3](PF_6)_2$.** The excitation transfer of the CT($Ru^{2+}$) to $Os^{2+}$ takes place without a couple of

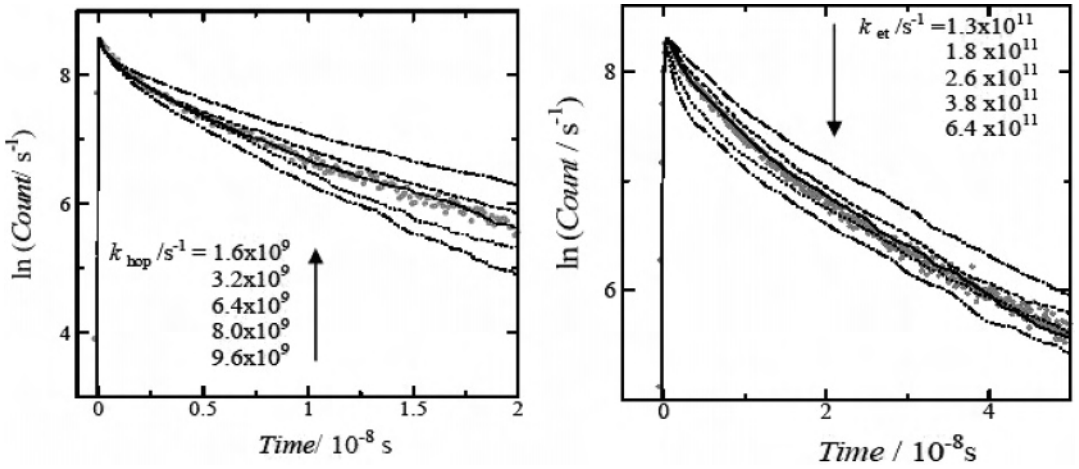


**Figure 8.** Simulated decay curves of $[Ru_{0.94}Os_{0.06}(bpy)_3](PF_6)_2$ (left) and $[Ru_{0.885}Os_{0.115}(bpy)_3](PF_6)_2$ (right) with a $\beta$ of 10 $nm^{-1}$ and a $k^0_{hop}$ of (1.6−9.6) × $10^{10}$ $s^{-1}$, and a $k^0_{et}$ of (1.3−6.4) × $10^{11}$ $s^{-1}$.

excitation hopping at the beginning of the decay, when the population of $Os^{2+}$ at the nearest sites and at the second-nearest sites increases. Any inhomogeneity of the $Os^{2+}$ moiety around the excited cations of $Ru^{2+}$ would add a multiexponential emission decay of the CT($Ru^{2+}$) to a single exponential one. The latter component of the decay is responsible for the excitation transfer to $Os^{2+}$ after the successive hoppings throughout the later time region. If excitation hopping were to take place successively even in the initial time, the number of the $Os^{2+}$ moiety would be averaged in an effective space that had been enlarged by the successive excitation hoppings. Multiexponential decay of the host emission of the $PF_6^-$ salt crystal containing $[Os(bpy)_3]^{2+}$ with a mole fraction of 0.06, 0.115, or 0.23 emerged in the first half of the emission decay.[7] A step-by-step Monte Carlo simulation of the emission decays of $[Ru_{0.94}Os_{x0.06}(bpy)_3](PF_6)_2$ and $[Ru_{0.885}Os_{x0.115}(bpy)_3](PF_6)_2$ was reexamined with the limiting rate constant $k^0_{et}$ of excitation transfer to an imaginary site at the van der Waals distance taken as a variable parameter. As Figure 8 shows, this variable parameter changes considerably the initial part of emission decay of the crystal that was doped with $Os^{2+}$ at a mole fraction of 0.115. It is very important to compare the simulated decay of the crystal doped with $Os^{2+}$ at a mole fraction of 0.0099 (part a of Figure 1). The rate of excitation transfer to an imaginary site at the van der Waals distance, 2.6 × $10^{11}$ $s^{-1}$, was obtained from the simulation of the emission decay of the crystal doped with $Os^{2+}$ at a mole (≈$10^{13}$ $s^{-1}$) fraction of 0.115. Meanwhile, the rate of excitation hopping varies the last half of the emission decay, and the limiting rate of excitation hopping to an imaginary site at the van der Waals distance is scattered (1.5 × $10^{11}s^{-1}$ for an $x$ of 0.115 and 0.64 × $10^{10}$ $s^{-1}$ for an $x$ of 0.06) compared with 0.64 × $10^{10}$ $s^{-1}$ determined before in the simulation of emission decays of the crystals doped with $Os^{2+}$ at a low fraction of 0.0099.

The limiting excitation transfer rate of 2.6 × $10^{11}$ $s^{-1}$ is smaller than those of nonadiabatic reactions of chemically bound donor−acceptor compounds by 2 orders of magnitude. This is reasonable because the population of a hole at the triplet MLCT state (α) is 0.20 in the occupied $\pi$ orbitals of ligands;[36] the square of hole super-exchange interactions between the neighboring cations is thought to be small (0.04).

**4. Diffusion Constants of Excitation Hopping in $[Ru_{1-x}Os_x(bpy)_3]X_2$ Crystals (X = $PF_6^-$ and $ClO_4^-$).** The sequential hopping of excitation results in a migration of excitation throughout the crystals. The diffusion constant of excitation along the $a$ axis of the crystal is given by the following equation,

$$D_a = \sum_j \frac{k_j d_{ja}^{\,2}}{2} \tag{12}$$

where $k_j$ and $d_{ja}$ are the total rates of hopping to the $j$-th closest site and the projection of length of the $j$-th closest hopping along the $a$ axis, respectively. The rate constants of hopping to the close sites via the electron-exchange mechanism are calculated from the limiting rate at the van der Waals distance $k^0_{hop}$, the interpyridyl distance, and the distance-attenuation factor $\beta$. The magnitudes of $D_a$ and $D_b$ (9.3 × $10^{-6}$ and 9.1 × $10^{-6}$ $cm^2$ $s^{-1}$, respectively) in the $PF_6^-$ salt crystal are calculated to be 6 times larger than $D_c$ (0.17 × $10^{-5}$ $cm^2$ $s^{-1}$) from the values of $k_j$ and $d_{jc}$, which are shown in Table 2. The small magnitude of $D_c$ comes from the small number of the neighboring cations and the small length of hopping compared with the diffusion along the $a$ and $b$ axes. No difference in the diffusion constants between the $a$ axis and the $b$ axis implies that the hopping takes place not via a dipole−dipole mechanism but via an exchange mechanism. The magnitude of the estimated diffusion constants are in the range of (1.4 −9.3) × $10^{-6}$ $cm^2$ $s^{-1}$, which is larger than that of the isotropic diffusion constant (1.3 × $10^{-6}$ $cm^2$ $s^{-1}$) that was roughly estimated in section 1.1 (Table 1). The magnitudes of $D_a$ and $D_b$ are twice as large as that of $D_c$ for the $ClO_4^-$ salt crystal, as shown in Table 6.

## Conclusion

Decay profiles of the triplet metal-to-ligand charge-transfer excited state in anisotropic crystals of $[Ru_{1-x}Os_x(bpy)_3]X_2$ (X = $ClO_4^-$, $PF_6^-$, $SbF_6^-$) were measured by means of time-

correlated single-photon counting. Dependence of the almost single-exponential decays of excited $[Ru(bpy)_3]^{2+}$ on the concentration of $Os^{2+}$ are interpreted by the occurrence of excitation hopping followed by the excitation transfer to $[Os(bpy)_3]^{2+}$. A step-by-step Monte Carlo simulation of the emission decays demonstrated that hopping rates calculated from the anisotropic interactions between transition dipoles of a donor and an acceptor for various configurations between neighboring cations in the crystals are insufficient to simulate the decay profiles. A step-by-step Monte Carlo simulation also demonstrated that the hopping to the cations of $[Ru(bpy)_3]^{2+}$ at the nearest and at the second-nearest sites via another interaction of super exchange between d orbitals through the bpys is the most essential, and the rates of the hopping are dependent on a distance-attenuation factor $\beta$ and the limiting rate of the excitation hopping to the imaginary neighboring cation at the van der Waals distance. It was determined that the value of the latter for the $[Ru_{1-x}Os_x(bpy)_3](ClO_4)_2$ at a mole fraction of 0.0099, 0.060, and 0.115 is $0.83 \times 10^{10}$ $s^{-1}$ on average by presuming a distance-attenuation factor $\beta$ of 10 $nm^{-1}$. Anisotropic diffusion constants estimated to be in a range of $(1.4-9.3) \times 10^{-6}$ $cm^2$ $s^{-1}$ from the hopping rates and the hopping lengths along the crystal axes are a little larger than an isotropic diffusion constant, $1.3 \times 10^{-6}$ $cm^2$ $s^{-1}$, calculated from the bimolecular excitation transfer rates on the basis of the isotropic Smoluchowski equation. Multiexponential decay of the emission of $[Ru_{0.885}Os_{0.115}(2,2'\text{-bipyridine})_3](PF_6)_2$ is also simulated to assess the limiting rate of excitation transfer to $[Os(bpy)_3]^{2+}$ at the van der Waals distance, $2.6 \times 10^{11}$ $s^{-1}$, using a step-by-step Monte Carlo method. The magnitude of $\beta$ determined is 6.5 and 11.5 $nm^{-1}$ for the $ClO_4^-$ and the $SbF_6^-$ crystals, respectively, on reference to the $\beta$ (10 $nm^{-1}$) for the $PF_6^-$ crystal.

The total rate of hopping to all of the neighboring sites at 298 K, $7.7 \times 10^9$ $s^{-1}$, is 380 times the hopping rate of excitation at a higher-energy site ($1.6 \times 10^7$ $s^{-1}$) to the lowest energy site in the $[Ru(bpy)_3](PF_6)_2$ at 1.3 K.[5] A large difference in the hopping rate between 298 and 1.3 K may be caused by an energy barrier (400 $cm^{-1}$) due to a vibrational reorganization energy (1600 $cm^{-1}$)[27] of the hopping. To investigate two possible mechanisms of barrier crossing and tunneling, studies of temperature effects on the hopping rate are now in progress.

**Acknowledgment.** We gratefully thank Emeritus Prof. Morton Z. Hoffman of Boston University for giving a lot of valuable comments on the manuscript of this article and for improving the English of the manuscript.

IC060948F